2019 16th International Conference on Electrical Engineering, Computing Science and Automatic Control (CCE)
Mexico City, Mexico. September 11-13, 2019

Interface Phenomena in Mn_xO_y/ZnO Thin Films for Oxide Electronics

Karen A. Neri-Espinoza
Doctorate in Nanoscience and Micro-Nanotechnology
ENCB, Instituto Politécnico Nacional
Mexico City, Mexico.
neri.karen8@gmail.com

Roberto Baca-Arroyo
Department of Electronics
ESIME, Instituto Politécnico Nacional
Mexico City, Mexico
rbaca02006@yahoo.com.mx

José A. Andraca-Adame
UPIIH
Instituto Politécnico Nacional
Pachuca Hidalgo, Mexico
andraca1@yahoo.com.mx

Ramón Peña-Sierra
Department of Electrical Engineering, SEES
CINVESTAV
Mexico City, Mexico
rpsierra@cinvestav.mx

***Abstract*— Interface phenomena in oxide electronics are of utmost importance due to the interactions that are present between the materials and can offer interesting electrical behavior for adaptive oxide devices. Thin films were synthesized on a Si (100) n-type substrate by Sputtering where the layers of manganese oxide are obtained through thermal oxidation at medium temperatures (T<500°C) and later on, a layer of ZnO:Zn is deposited. X-Ray Diffraction (XRD) and Raman spectroscopy are done to investigate the structure of the Mn; the layers of manganese exhibit different phases of oxidation caused by the thermal process. To study the interface phenomena, an electrical characterization (current – voltage curves) is done to understand what happens in the interface of Mn_xO_y/ZnO. In one of the IV curves obtained of a ZnMnSi structure, a similar curve to the characteristic one of a diode is observed, thus, this work intends to demonstrate the use of Mn and Zn as important metals for oxide electronics and the development of electronic adaptive devices.**

Keywords—Interface, Mn, ZnO, Sputtering, Adaptive oxide electronics.

I. INTRODUCTION

Manganese oxides (MO) continue to be materials of technological importance for environmental remediation, catalytic and electrochemical applications, and also to produce soft magnetic materials such as Mn-Zn ferrite [1], [2]. MO of different structure (MnO, Mn_2O_3, MnO_2, and Mn_3O_4) are usually prepared by varying calcination conditions of starting chemical precursors from bulk or film. In natural environments, manganese (Mn) occurs in the Mn^{2+}, Mn^{3+}, and Mn^{4+} oxidation states in octahedral coordination with O^{2-} [3].

ZnO is a well-known and used material in the nanomaterials area, especially for the construction of different electronic devices such as transparent semiconductors, sensors, transistors, etc. [4]. A ZnO:Zn layer presented in this work will allow investigating other features not found on a pure ZnO film that has been reported several times before [5]–[10].

Lastly, physics studies on many functional metal oxides suggest that properties, like resistivity, polarization and magnetization can be modified electrically as a non-volatile adjustable state (stable condition)[11]. Such devices are identified as adaptive oxide electronics, which may be possible to implement, hence, expanding the potential for electronics in general [12]. To demonstrate that materials as MOs and ZnO have been considered primarily for other applications where they may also have utility in emerging adaptive oxides [13], interface phenomena from manganese and zinc oxides grown onto Si must be regarded more broadly, given that appropriate orientation and properties at the surface in Si must be taken into account [14], [15].

II. EXPERIMENTAL PROCEDURE

A. Substrate and Mn deposition conditions

The synthesis process is crucial to obtain the features that are desired in the device.

Cleaning the substrates is of extreme importance to obtain homogeneous and uniform thin films. Before the deposition, Si (100) n-type wafers (of approximately 300-350 µm of thickness) were cleaned with xylene, acetone, and propanol with cycles of 15 min each in an ultrasonic cleaner. After this process, the substrate is ready for the sputtering deposition.

A manganese (Mn) target (99.9%) is used with a DC Magnetron for the deposition. The conditions used are 30 W and 5 SCCM (Standard Cubic Centimeters per Minute) of Ar. The vacuum pressure varied from 3.5 – 4 mTorr. For these experiments, the deposition rate of Mn was 0.2 - 0.3 KÅ/s where the final thickness of the film is around 100 nm.

B. Thermal oxidation

To obtain the different phases of oxides of the materials, thermal oxidation was carried out at 250 °C, 350 °C and 450 °C in air atmosphere. Fig. 1 shows the structure for this process.

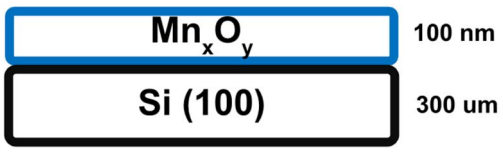

Fig. 1. Structure for the deposition of Mn samples named MnSi.

The nomenclature to identify the samples and times used in the oxidation are tabulated in TABLE I.

978-1-7281-4840-3/19/$31.00 ©2019 IEEE

TABLE I. NOMENCLATURE OF THE SAMPLES AND OXIDATION CONDITIONS

Name	T (°C)	Time (min)
MnSi-1	25	-
MnSi-2	250	90
MnSi-3	350	90
MnSi-4	450	90

The samples were characterized by X-Ray Diffraction (XRD) with a PANalytical X'Pert Pro diffractometer of CuKα (λ = 0.15418 nm) in the scan range of 20-60°. Raman bands were performed by Micro-Raman System (Horiba Jobin-Yvon, HR800) with excitation line λ = 632.8 nm (He-Ne laser) at 20mW in the range of 100-800 cm^{-1}.

C. ZnO:Zn deposition

After the oxidation and characterization process of the manganese films, a layer of ZnO:Zn is deposited. The structure obtained is appreciated in Fig. 2.

For the ZnO:Zn layer, a co-sputtering was done and the conditions of the different targets are the following:
ZnO: 99.999% purity, RF magnetron, 125 W.
Zn: 99.999% purity, DC magnetron, 5 W.
Both at 10 SCCM of Ar and with a pressure of 5 – 5.3 mTorr. The thickness of this film is also of 100 nm. Finally, the names of the samples will be given as ZnMnSi-1, ZnMnSi-2, ZnMnSi-3, and ZnMnSi-4 related the TABLE I for the double-layer structure.

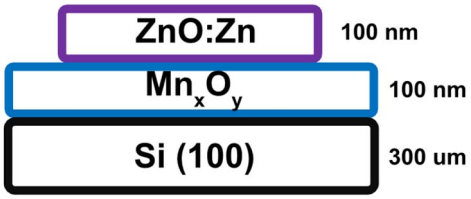

Fig. 2. Final structures with two layers, the first one of Mn with thermal oxidation and a ZnO:Zn as the last one. The samples are named ZnMnSi.

For the interface phenomena of the final structure, the electrical behavior of the samples was provided by current-voltage curves collected with a digital storage oscilloscope (Keysight, EDUX1002G). A function generator integrated into the oscilloscope is also employed to produce a sinusoidal signal at low frequency (f = 100 Hz) with voltage scanned from -1V to 1V.

III. STRUCTURAL CHARACTERIZATION

A. X-Ray Diffraction (XRD)

Fig. 3 shows the XRD patterns of the analyzed samples. The samples exhibit oxide phases such as MnO (cubic) and Mn_3O_4 (tetragonal, spinel). The crystallographic charts (as well as their type) that were used to compare the peaks are:

- MnO: 01-075-0626 (Calculated)
- Mn_3O_4: 00-024-0734 (Star)

The evolution of the samples is the following: without thermal oxidation, 250 °C and 350 °C, the MnO phase is constant; It is at 450 °C that the Mn_3O_4 phase occurs which was also observed in the results of Raman spectroscopy. The lack of more peaks in the MnSi-4 sample may well be because the deposited and oxidized material is conforming to the substrate.

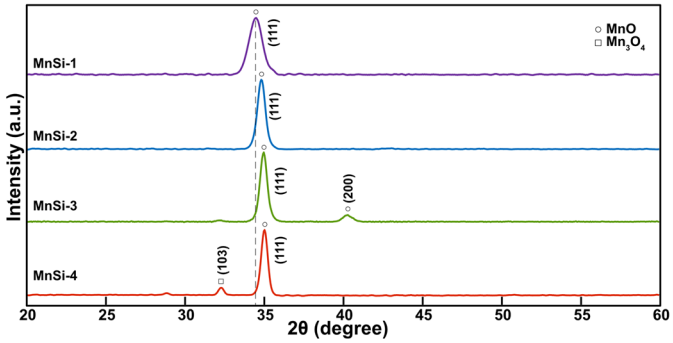

Fig. 3. X-ray diffraction patterns of the MnSi samples.

B. Raman spectroscopy

Raman spectroscopy is a sensitive tool to probe the short-range environment of oxygen coordination (O^{2-}) around transition metal cations in oxide lattices, such as Mn^{2+} and Mn^{3+} in an MO structure. Fig. 4 shows the Raman spectra of the samples. Raman bands and attributed vibrational modes are listed in TABLE II [16], [17].

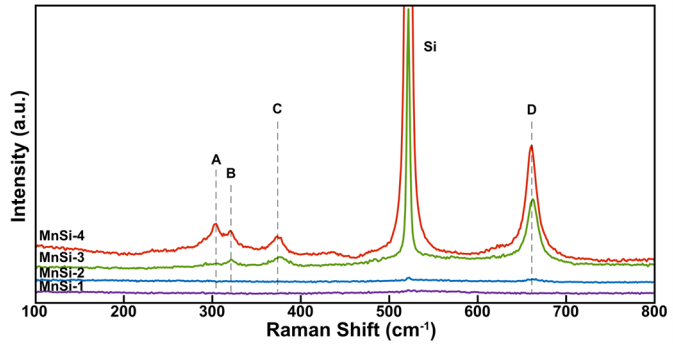

Fig. 4. Raman spectroscopy of the MnSi samples.

TABLE II. RAMAN BANDS AND VIBRATIONAL MODES OF THE SAMPLES

Band	Position	Vibrational mode
A	298 – 309	F_{1u}
B	317 – 323	E_g
C	363 – 382	$F_{2g}^{(3)}$
D	640 – 680	A_{1g}

In samples MnSi-1 and MnSi-2 there is no visible Raman activity. For the A band, the ordering featured in MnO_6 bonding is due to the native MnO phase formation [18].
For MnSi–3, the bands B and C, related to the Mn_3O_4 phase, begin to form. Band D is more defined than the other bands and this is related to the Jahn – Teller effect. Finally, for the MnSi–4 sample, the four bands (A, B, C, and D) are defined and the

phase Mn_3O_4 exist due to Jahn – Teller coupling of the Mn^{3+} ion, because cations occupy the octahedral B-site (Mn^{3+}) and tetrahedral A-site (Mn^{2+}) corresponding to a normal spinel structure [19]; its presence increases with a higher temperature. The D band corresponds to the Mn-O stretching vibrations and is associated with the Mn^{3+} ions [17].

IV. INTERFACE PHENOMENA

Obtaining current-voltages (IV) curves allow to recognize the behavior of the film at a frequency and with different types of signal. According to the signal that is seen, this can be compared with the forms already known and understand the behavior tendency of the device. The samples were standardized to be about 1 cm by 1 cm.

Fig. 5 displays the IV curves of the structures, as well as a comparison of the response of a pure Si (100) wafer (of 1 cm^2 too). The response is transversal to the structure, in which it will be possible to discuss the interface phenomena of the final device.

The Si (100) has a linear response that corresponds to a resistor, to compare the effects of Mn and Zn (and its oxides) in the structure, Fig. 5 shows the comparison of the films.
For Fig. 5 a), we observe that the response between the Si and MnSi-1 (no thermal oxidation) is very similar and linear. But, in the structure ZnMnSi-1 the story changes, the curve that can be seen is comparable to the behavior of a diode, meaning that a structure of just two layers (MnO and ZnO:Zn) of 100 nm can exhibit such response. Of course, this occurs as a result of the MnO/ZnO:Zn interface, given that the MnSi-1 does not behave in that manner. In Fig. 6 a time-domain signal for the ZnMnSi-1 can be observed and it clearly shows the diode behavior that was mentioned.

To observe the effect of the temperature at the interface, Fig. 5 b) to 5 d) are shown. For Fig. 5 b), the layer of Mn also indicates an MnO phase. For the MnSi-2, the response is similar to the sample without thermal oxidation; the ZnMnSi-2 changes and now manifest an almost linear response with a larger resistance as the signal drops below 0.5 μA.

Fig. 5 c) now illustrates the response of the 350 °C process. MnSi-3 has a non-linear curve where an ellipsoid can be observed; this phenomenon indicates a phase displacement of the signal in relation to the input signal (V_{in}); the shift can be attributed to the strain that exists between the Si and the MnO (as seen in a displacement of the XRD peak of Fig. 4). For the ZnMnSi-3 the response is linear with more conductivity than MnSi-3.

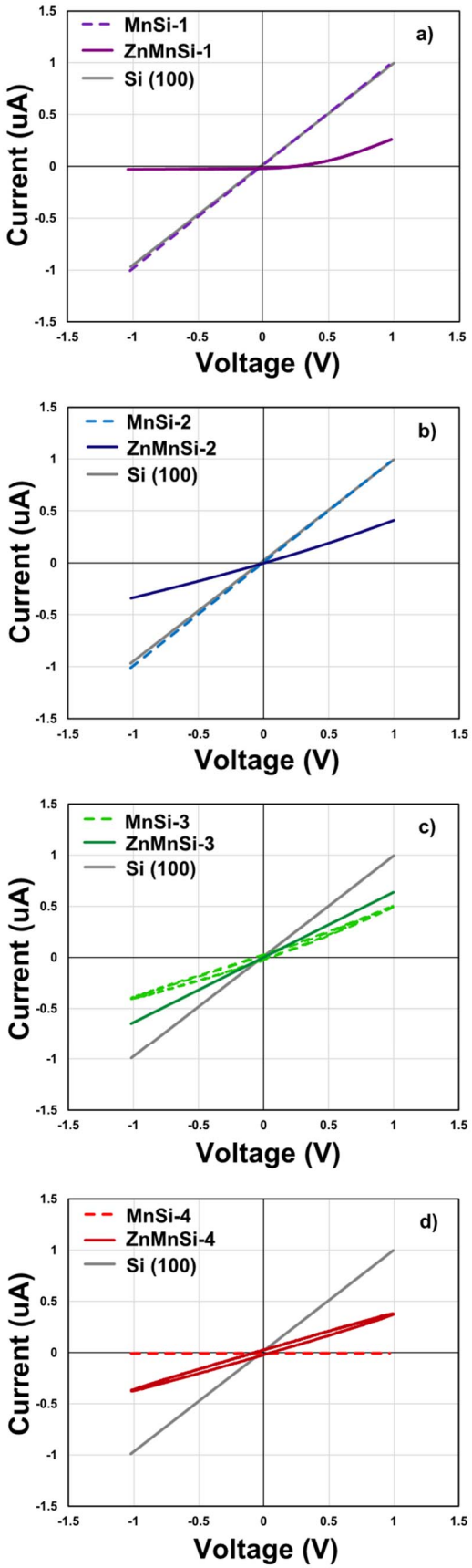

Fig. 5. Current-voltage transversal curves of the different structures.

In Fig. 5 d), the MnSi-4 according to the evidence of XRD, has a mixture of a Mn_3O_4 (spinel) and MnO. The structure of this layer becomes non-conductive, and the response can be seen where no current is flowing (line in the zero axis). For the ZnMnSi-4, there is a surprisingly non-linear response like in MnSi-3 where a phase displacement also exists. The word surprise refers to the difference of having an insulator layer (MnSi-4) transforming into a conductive structure (ZnMnSi-4). No doubt this is a noteworthy transition and an important proof of the relevance of interface phenomena, given that all these behaviors exist because of an interface between the materials and substrate.

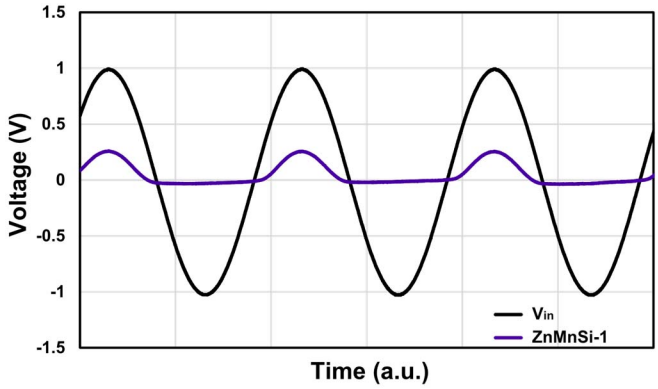

Fig. 6. The signal observed in the time domain for the ZnMnSi-1 structure. V_{in} is a sinusoidal signal of 100 Hz. The response is attenuated but the structure acts as a diode and the signal obtained is a typical half-wave rectifier.

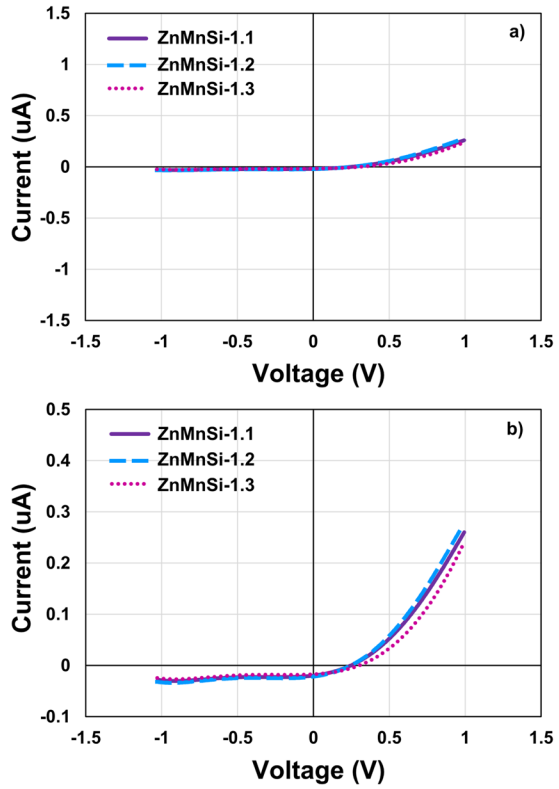

Fig 7. Current-voltage curves to test the reproducibility of the ZnMnSi-1 structure.

Finally, Fig. 7 demonstrates the response of three ZnMnSi-1 structures to test the reproducibility of the thin films, where, the process of synthesis was done from the start for every sample and it confirms that the behavior observed is given by the interface of ZnMn. For Fig. 7 a), the scale used is the same from Fig. 5 curves to facilitate comparison; in Fig. 7 b), a reduced scale is established to distinguish the variation between the structures where it reveals little deviations between signals but the tendency of the diode-type response continues.

V. CONCLUSIONS

The conditions of Mn thin films deposited by Sputtering are presented. Manganese oxides (MO) have been obtained by a thermal oxidation process in an air atmosphere at different temperatures. The structural characterization of the films shows the presence of two Mn phases: MnO (cubic) and Mn_3O_4 (spinel).

MnO forms even without thermal oxidation, as we can see in the XRD results, this is important due to the structure of ZnMnSi-1 that has an electrical response typical of a diode. The film does not go through thermal oxidation, meaning a device such as a thin film diode can be obtained simply by the deposition of these consecutive layers.

Also, we observed a surprising response of the ZnMnSi-4 sample, where previous to the deposition of ZnO:Zn (MnSi-4) it behaves as an insulator and after the Zn deposition it changes to a conductive structure with certain resistivity that attenuates the signal. This will be further analyzed in future investigations.

In summary, Zn and Mn structures (which can be called ZMO for future references) are of great interest for oxide electronics and the development of electronic adaptive devices given that the interface phenomena between layers do have several remarkable responses that are useful for electronics devices.

ACKNOWLEDGMENT

The authors acknowledge financial support from the *Consejo Nacional de Ciencia y Tecnología* (CONACyT, México). Also, this work has been possible thanks to the technical support of MSc. Miguel Galván Arellano, MSc. Adolfo Tavira Fuentes and professional Norma Iris González García of the *Centro de Investigación de Estudios Avanzados del Instituto Politécnico Nacional* (CINVESTAV-IPN, México).

REFERENCES

[1] C. E. Frey *et al.*, "Evaporated manganese films as a starting point for the preparation of thin-layer MnO: X water-oxidation anodes," *Sustain. Energy Fuels*, vol. 1, no. 5, pp. 1162–1170, 2017.

[2] H. Jamil, M. Khaleeq-Ur-Rahman, I. M. Dildar, and S. Shaukat, "Structural and optical properties of manganese oxide thin films deposited by pulsed laser deposition at different substrate temperatures," *Laser Phys.*, vol. 27, no. 9, 2017.

[3] A. H. Reidies, "Manganese Compounds," in *Ullmann's Encyclopedia of Industrial Chemistry*, Weinheim: Wiley-VCH Verlag GmbH & Co. KGaA, 2012, p. 22.

[4] S. J. Pearton, D. P. Norton, K. Ip, Y. W. Heo, and T. Steiner, "Recent progress in processing and properties of ZnO," *Prog. Mater. Sci.*, vol. 50, no. 3, pp. 293–340, 2005.

[5] C. N. Chinnasamy, A. Narayanasamy, N. Ponpandian, K. Chattopadhyay, H. Guérault, and J. M. Greneche, "Magnetic

properties of nanostructured ferrimagnetic zinc ferrite," *J. Phys. Condens. Matter*, vol. 12, no. 35, pp. 7795–7805, 2000.

[6] S. Lany, "Semiconducting transition metal oxides," *J. Phys. Condens. Matter*, vol. 27, no. 28, p. 283203, 2015.

[7] F. Rubio-Marcos *et al.*, "Some clues about the interphase reaction between ZnO and MnO2 oxides," *J. Solid State Chem.*, vol. 182, no. 5, pp. 1211–1216, 2009.

[8] Y. Leprince-Wang, "Properties of ZnO," *Piezoelectric ZnO Nanostructure Energy Harvest.*, pp. 1–19, 2015.

[9] R. Baca *et al.*, "Kinetics of the oxidation of Zn foils in air atmosphere," *IOP Conf. Ser. Mater. Sci. Eng.*, vol. 8, p. 012043, 2010.

[10] L. Yi *et al.*, "The photo- and electro-luminescence properties of ZnO:Zn thin film," *Displays*, vol. 21, no. 4, pp. 480–482, 2000.

[11] J. Cao and J. Wu, "Strain effects in low-dimensional transition metal oxides," *Mater. Sci. Eng. R Reports*, vol. 71, no. 2–4, pp. 35–52, 2011.

[12] S. D. Ha and S. Ramanathan, "Adaptive oxide electronics: A review," *J. Appl. Phys.*, vol. 110, no. 7, 2011.

[13] R. Baca, "Manganese oxide thin-films for current-signal sensing and thermal insulation," *Mater. Sci. Semicond. Process.*, vol. 16, no. 5, pp. 1280–1284, 2013.

[14] F. M. Zhang *et al.*, "Investigation on the magnetic and electrical properties of crystalline Mn0.05Si0.95 films," *Appl. Phys. Lett.*, vol. 85, no. 5, pp. 786–788, 2004.

[15] S. Sze and K. K. Ng, *Physics of Semiconductor Devices*, 3rd Ed. John Wiley & Sons, 2007.

[16] T. Gao, H. Fjellvåg, and P. Norby, "A comparison study on Raman scattering properties of α- and β-MnO2," *Anal. Chim. Acta*, vol. 648, no. 2, pp. 235–239, 2009.

[17] C. M. Julien and M. Massot, "Raman spectroscopic studies of lithium manganates with spinel structure," *J. Phys. Condens. Matter*, vol. 15, no. 19, pp. 3151–3162, 2003.

[18] C. Julien, M. Massot, S. Rangan, M. Lemal, and D. Guyomard, "Study of structural defects in γ-MnO2 by Raman spectroscopy," *J. Raman Spectrosc.*, vol. 33, no. 4, pp. 223–228, 2002.

[19] D. P. Dubal, D. S. Dhawale, R. R. Salunkhe, and C. D. Lokhande, "Conversion of interlocked cube-like Mn3O4 into nanoflakes of layered birnessite MnO2 during supercapacitive studies," *J. Alloys Compd.*, vol. 496, no. 1–2, pp. 370–375, 2010.